Predictive mapping of soil electrical conductivity as a Proxy of soil salinity in south-east of Algeria

Article *in* Environmental and Sustainability Indicators · December 2020

DOI: 10.1016/j.indic.2020.100087

CITATIONS
0

READS
189

8 authors, including:

Abdennour mohamed amine
Université de Biskra
15 PUBLICATIONS **18** CITATIONS
SEE PROFILE

Douaoui Abdelkader
Tipaza University Center (Algeria)
92 PUBLICATIONS **746** CITATIONS
SEE PROFILE

Chiara Piccini
CREA - Council for Agricultural Research and Economics
45 PUBLICATIONS **259** CITATIONS
SEE PROFILE

Manuel Pulido
Universidad de Extremadura
49 PUBLICATIONS **624** CITATIONS
SEE PROFILE

Environmental and Sustainability Indicators 8 (2020) 100087

Contents lists available at ScienceDirect

Environmental and Sustainability Indicators

journal homepage: www.journals.elsevier.com/environmental-and-sustainability-indicators/

Predictive mapping of soil electrical conductivity as a Proxy of soil salinity in south-east of Algeria

Mohamed Amine Abdennour [a,*], Abdelkader Douaoui [b], Chiara Piccini [c], Manuel Pulido [d], Amel Bennacer [e], Abdelhamid Bradaï [f], Jesús Barrena [d], Ibrahim Yahiaoui [b]

[a] Laboratory of Ecosystem Diversity and Agricultural Production System Dynamics in Arid Zones (DEDSPAZA), Mohamed Khider University, Biskra, 07000, Algeria
[b] Laboratory of Crop Production and Sustainable Valorization of Natural Resources, Djilali Bounaama University, Khemis Miliana, 44225, Algeria
[c] Council for Agricultural Research and Economics, Research Centre for Agriculture and Environment, Via Della Navicella 2–4, 00184, Rome, Italy
[d] GeoEnvironmental Research Group, University of Extremadura, Cáceres, 10071, Spain
[e] Laboratory of Valorization and Conservation of Biological Resources, Faculty of Sciences, Mohamed Bougara University, Boumerdes, BP, 35000, Algeria
[f] Laboratory of Water and Environment, Hassiba Ben Bouali University, Chlef, 02180, Algeria

ARTICLE INFO

Keywords:
Ordinary kriging
Cokriging
Indicator kriging
Spatial variability
Saturation index
Biskra

ABSTRACT

In semi-arid and arid areas soil salinity has adverse effects both on the environment and agricultural production. The region of Biskra (South-East of Algeria) underwent a strong agricultural transformation from traditional oasis agriculture to an almost exclusive production of dates involving market gardening throughout the year. The main goal was to predict the spatial variation of EC using geostatistics and a Geographic Information System (GIS), comparing also the performance of two classical geostatistical interpolators - Ordinary Kriging (OK), using only point data, and Cokriging (CK), introducing also auxiliary variables to improve prediction accuracy (SI gypsum and SO_4^{2-}, obtained from the analysis of the chemical and geochemical processes of soil salinization). For this study, a total of 42 soil samples were randomly collected from topsoil (0–15 cm) in the irrigated perimeter of El Ghrous, a representative rural community located in the west of Biskra. Aiming to better understand the processes that most influence the evolution of soil salinity in this area, some chemical parameters were determined, among which the electrical conductivity (EC). Moreover, some terrain parameters were derived from a digital elevation model as auxiliary information, and Normalized Difference Vegetation Index (NDVI) was calculated from satellite imagery. The prediction efficiency of the methods was evaluated by calculating the mean error (ME) and the root mean square error (RMSE). The resulting maps showed that soils in the study area are affected by salinization. Cross-validation results showed a better performance in estimating EC of CK, after the introduction of the covariates, than OK, with an RMSE value of 0.92 vs. 1.53. This suggests a greater efficiency of CK in EC prediction in this area, confirming that the introduction of some auxiliary data correlated to the target variable significantly improves the interpolation. A third kriging technique, Indicator Kriging (IK) was applied to generate a map of the probability of exceeding a given threshold.

1. Introduction

Understanding how soil properties vary in space is a key issue for making fair decisions within a framework of sustainable agriculture (Norouzi et al., 2010; Chagas et al., 2018). In the particular case of the province of Biskra (South-East of Algeria) the arid conditions have forced farmers to use groundwater for irrigation, but the utilized groundwater not always has an acceptable quality. This influences largely both soil quality and crop yields, leading to land degradation in several cases, as well as the agricultural development (Boufekane and Saighi, 2016; Adimalla and Taloor, 2020).

The Biskra region is characterized by a strong phonicicultural potential (date palm) with more than 5 million date palms and nearly 100,000 water points (wells and boreholes) (Rechachi, 2017). All these potentials constitute a factor of progress and improvement of the living conditions of the local population and food satisfaction at the country level (Rechachi, 2017). Unfortunately, this achievement is threatened by an irrational management of the resources, particularly the soil. Agricultural land surface in the region of Biskra has increased from 87,187 ha in 2008 to 105,927 ha in 2015, i.e. an increase of 17.5% according to the

* Corresponding author.
E-mail address: ma.abdennour@univ-biskra.dz (M.A. Abdennour).

https://doi.org/10.1016/j.indic.2020.100087
Received 16 May 2020; Received in revised form 2 November 2020; Accepted 19 November 2020
Available online 24 November 2020

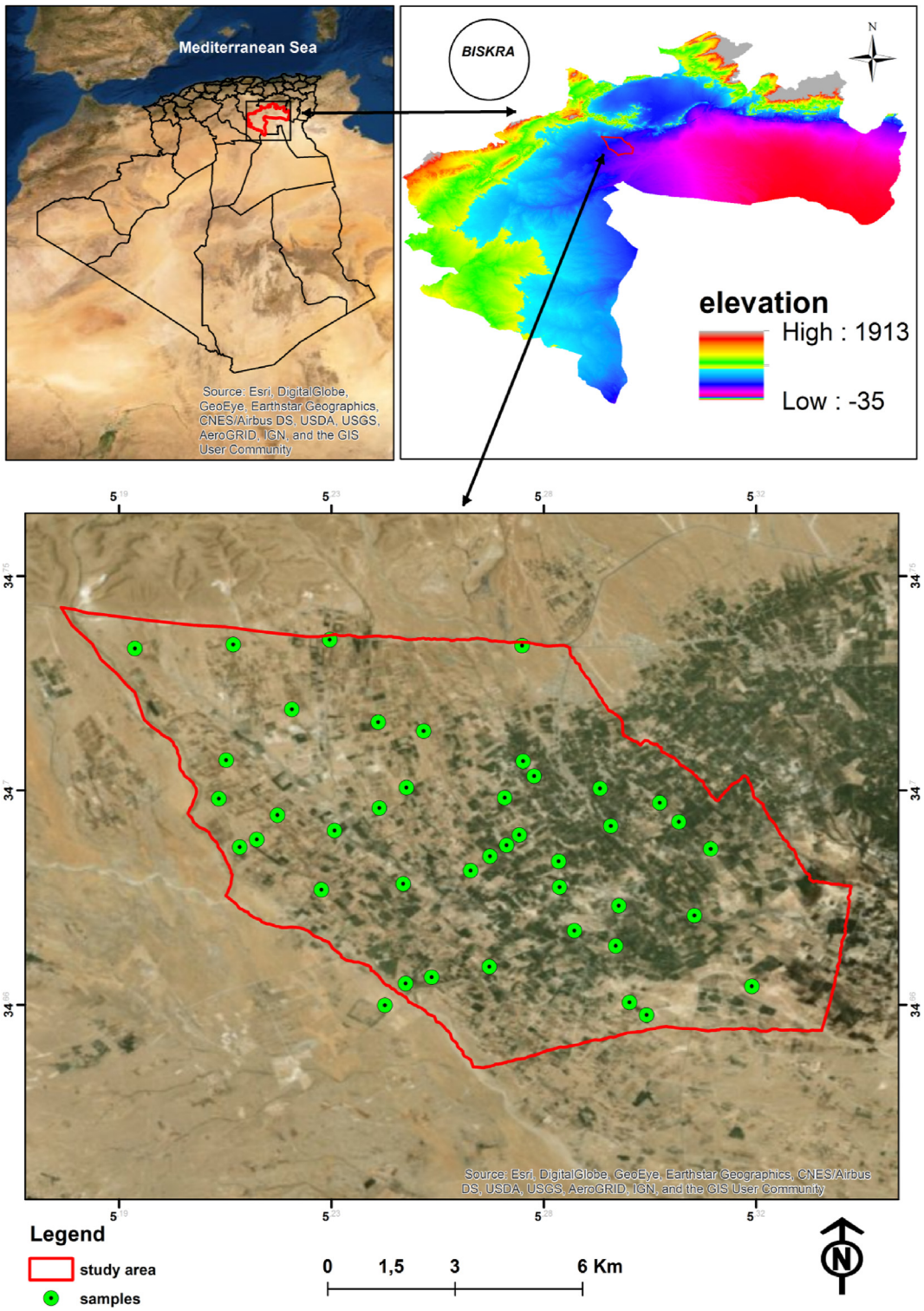

Fig. 1. Geographical location of the study area and Digital Elevation Model of the region.

Directorate of Agricultural Services (DSA). A worrying problem of soil salinization has been recently detected (Afrasinei et al., 2017; Abdennour et al., 2019b), by far the most serious problem for the irrigated agriculture of the region (Fourati et al., 2017; Gorji et al., 2017; Vermeulen and Van Niekerk, 2017).

In this region uncontrolled irrigation with groundwater of poor quality and by inadequate methods poses problems of management and conservation of soil and water resources, mainly related to hydro-geochemical dynamics. As a result, irrigation can either mobilize the salts initially present in the soil or bring them to the soil itself. In both cases, soil degradation can occur. From this point of view, the perimeter of El Ghrous presents a certain diversity of situations inducing an important spatio-temporal dynamics of soil salinization, which would be difficult to follow and to characterize. Since the 1990s, the El Ghrous region has undergone a major agricultural transformation, within the framework of the National Agricultural Development Plan, with many investment projects subsidized for young people. This change in land use will undoubtely have negative repercussions on the soil, mainly in the

Table 1
Statistical summary of physicochemical parameters.

Parameter	Min	Max	Mean	SD	CV
Ca^{2+} (meq l^{-1})	8.0	76.9	32.2	14.4	41.6
Mg^{2+} (meq l^{-1})	0.7	25.4	9.1	5.1	56.3
Na^{+} (meq l^{-1})	1.1	36.3	10.8	6.5	60.5
K^{+} (meq l^{-1})	0.0	2.7	0.5	0.5	87.0
Cl^{-} (meq l^{-1})	1.2	19.3	6.5	3.0	45.6
SO_4^{2-} (meq l^{-1})	2.8	50.5	14.0	6.7	47.5
HCO_{3^-} (meq l^{-1})	0.8	11.5	2.5	1.3	50.0
EC (dS m^{-1})	0.5	6.5	1.9	0.9	47.4
pH	7.7	8.9	8.1	0.2	2.7

form of salination and degradation of its structure. Afrasinei et al. (2017) applied remote sensing techniques for the assessment of soil salinity and degradation in a monitoring study carried out in the province of Biskra, where the perimeter of El Ghrouss is located. Following their land-use maps, obtained from a supervised classification, plots and areas within the irrigated perimeter of El Ghrous were classified as very saline.

Soil salinization has been studied worldwide (Pozdnyakova and Zhang, 1999; Douaoui et al., 2006; Yahiaoui et al., 2015; Taghizadeh-Mehrjardi et al., 2016; Niñerola et al., 2017; Wang et al., 2018; Semar et al., 2019). Some factors have been already agreed as drivers: (i) topographical position (Manning et al., 2001), (ii) soil type, and (iii) precipitation (Juan et al., 2011b). Moreover, the electrical conductivity (EC) can be influenced by physical (e.g., elevation) and chemical (e.g., pH, mineralogy) factors. The combined influence of one or more of these factors is what determines the level of salinity at a given location, and hence salinity variation across the landscape (Odeh and Onus, 2008).

Yahiaoui et al. (2015) found an interesting statistical relationship between soil salinity (measured by EC) and topography parameters, with which they could improve the predictive accuracy of soil salinity in the Low-Cheliff plain (Algeria). In this line, Vermeulen and Van Niekerk (2017) stated about the possibility of predicting soil salinity through a combination of multiple factors, including topographical features and machine learning algorithms. The variation in the geochemical composition of soil solutions is mainly a function of the interaction between groundwater and the mineral composition of these soils. Hence, several different methodologies have been applied to study, characterize and evaluate the sources of variation in salinity of irrigated soils, and different authors have tried to improve the accuracy of salinity prediction. While many researchers have opted for topographic factors (elevation, slope, etc.) (Florinsky et al., 2000; Yahiaoui et al., 2015; Fourati et al., 2017), others have used GIS and high-resolution satellite images (Eldeiry and Garcia, 2010; Gorji et al., 2017). They tried to find a correlation between EC and some spectral indices, lately through artificial intelligence algorithms. Not all these techniques are suitable for all regions, because of the differences in vegetation, soil type and ecology; in our study we tried to find a suitable technique for our region.

These spatial variations and interrelationships between variables related to soil salinity, such as dominant ions or topography are still of high complexity (Juan et al., 2011b). Thus, their comprehensive understanding is helpful for risk assessment and for the resolution of environmental problems (Florinsky et al., 2000). In addition, the traditional EC measurement method (saturated paste) is a time-consuming process. So, there is still a need to explore spatial estimation methods for mapping soil properties, using adequate and efficient tools such as GIS and geostatistics, for a better land/water management within a context of precision agriculture.

In the last 15 years research has focused both on probabilistic (stochastic) methods such as geostatistics and digital soil mapping to enable predictive models that takes into account soil heterogeneity and spatial variability from observed points in an known area (Hengl et al., 2007; Dankoub et al., 2012; Long et al., 2014; Zolfaghari et al., 2015; Azadmard et al., 2018; Boubehziz et al., 2020). Kriging, which indicates a series of interpolation algorithms proper of geostatistics, uses models of spatial correlation to estimate values in non sampled locations starting from measured point data (Goovaerts, 1997; Castrignanò et al., 2002; Safarbeiranvnd et al., 2018; Seyedmohammadi and Matinfar, 2018).

Table 2
Coefficients of correlation (Pearson's r) between EC and chemical parameters.

	Ca^{2+}	Mg^{2+}	Na^{+}	K^{+}	SO_4^{2-}	Cl^{-}	HCO_{3^-}	NO_{3^-}	pH
EC	0.69*	0.34	0.47	0.11	0.74*	0.44	0.36	0.49	0.29

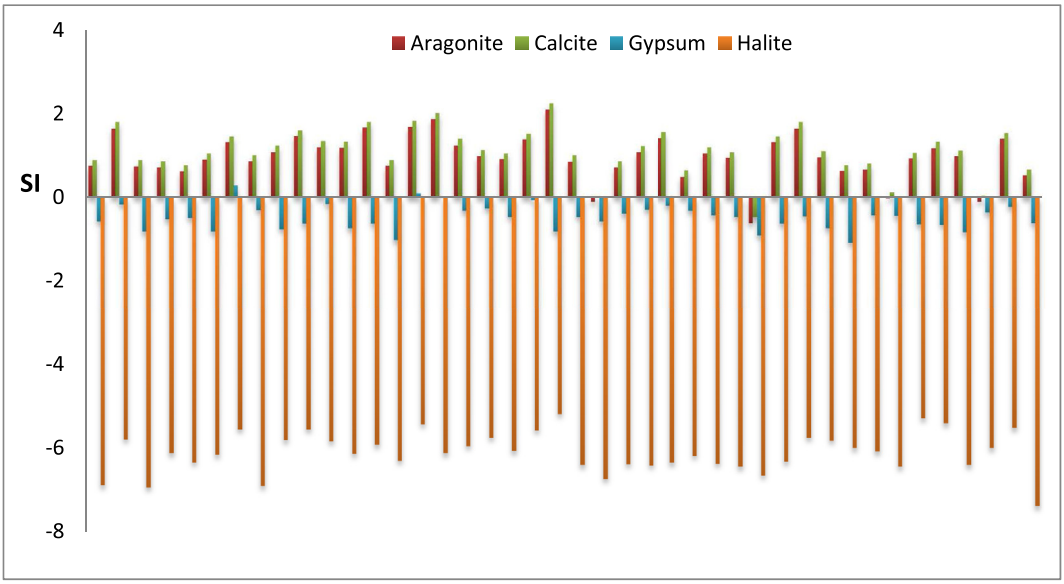

Fig. 2. Values of the saturation index of the main minerals.

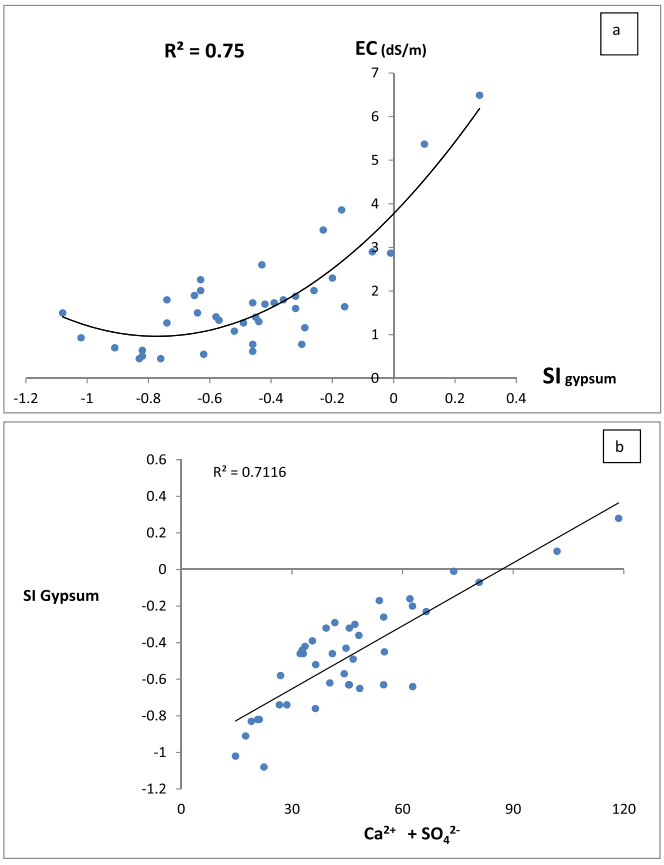

Fig. 3. Relationships between SI (gypsum) and EC (a); SI (gypsum) and $Ca^{2+} + SO_4^{2-}$ (b).

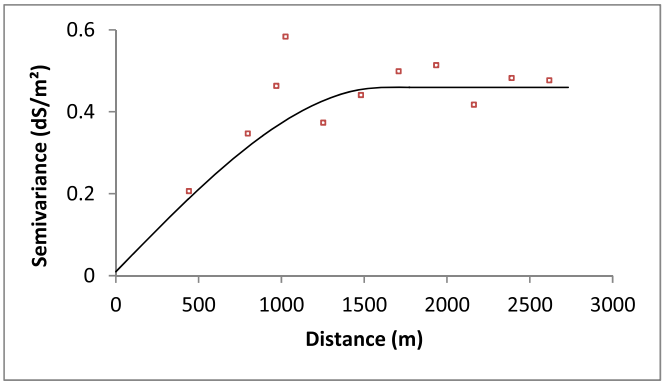

Fig. 4. Omnidirectional variogram of the predicted EC (OK).

Table 3
Coefficients of correlation (Pearson's r) between EC soil parameters and NDVI.

	EC	*DEM*	*Slope*	*NDVI*
EC	1.00			
DEM	**- 0.20**	1.00		
Slope	- 0.08	0.31	1.00	
NDVI	- 0.01	0.01	- 0.13	1.00

Several researchers have studied soil salinity through the application of different Kriging techniques, of which Ordinary Kriging (OK) is the most common. For instance, in United States (USA) Eldeiry and Garcia (2010) used OK to map soil salinity in Arkansas River Basin in southern Colorado, and Abdennour et al. (2019b) used the same type of Kriging to identify spatial variability of soil salinity in Biskra. Niñerola et al. (2017) have demonstrated the benefit of using OK for mapping soil properties. However, the precision of this method is limited, because it does not take into account other variables which would otherwise improve the interpolation results (Boubehziz et al., 2020). Another type of Kriging, Cokriging (CK), uses multiple correlated datasets, usually leading to a more accurate prediction. CK is an extension of OK from a single spatial random variable to two or more spatially correlated random variables (Tajgardan et al., 2010; Bogunovic et al., 2017). The value of the target variable at an unsampled location is estimated as a linear combination of the observed values of all available variables (Ashrafzadeh et al., 2016). Moreover, non-parametric geostatistical methods allow to estimate the probability that the true value of a soil property at an unsampled location exceeds a specified threshold, depending on observations at sampled sites (Lark and Ferguson, 2004). The main technique used for this purpose is Indicator Kriging (IK), widely applied by soil scientists (Van Meirvenne and Goovaerts, 2001; Lark and Ferguson, 2004; Piccini et al., 2012).

In this work we introduced a geochemical parameter, the saturation index (SI) as a possible covariate in CK, to improve the quality of estimation with a reduced number of samples. Values of such index, which depends on the interaction between soil mineral part and irrigation water brought to the soil, can be strongly influenced by the spatial evolution of salinity. Geochemical parameters represent very important indicators in studying salinity, since some minerals can dissolve and other can precipitate into the soil, and this will influence the EC.

The objectives of this study were: (i) to estimate soil EC in the study area, (ii) to analyze the spatial variability of EC at the irrigated perimeter scale by using geostatistics, (iii) to examine the ability of auxiliary information to improve the estimation accuracy by comparing two different methods (OK and CK), and (iv) to map the probability of exceeding a given threshold by IK, to individuate areas potentially prone to salinity. In attempting to improve the precision of the estimate by OK, we applied CK introducing as covariates (i) a physical parameter (elevation), (ii) a chemical parameter (SO_4^{2-}), and (iii) a geochemical parameter (saturation index for gypsum, SIg).

2. Materials and methods

2.1. Study area

This study was conducted in the region of El Ghrous in the province of Biskra, SE Algeria (Fig. 1). The community of El Ghrous belongs to the zone of Zab Elgharbi, which is 47 km from Biskra city. The Biskra region constitutes a pivotal zone between the north and the south of Algeria, and can be considered a transition zone from the morphological and bioclimatic point of view. This passage takes place suddenly at the foot of the Saharan Atlas, where we pass from a fairly high and rugged relief in the north to a plateau topography slightly sloping towards the south (Bougherara and Lacaze, 2009). El Ghrous is characterized by a Saharan climate with an average annual rainfall of 138 mm. The average annual values of temperature and relative humidity are respectively 22.3 °C and 42.9%.

The Biskra region represents a structural and sedimentary transition zone. Its northern part is mountainous, while the southern one is a collapsed area - part of the northern Sahara. The transition between these distinct domains occurs through a set of flexures, folds and faults of prevalent E-W orientation, called "accident south atlasique" (Chebbah, 2016). The region is mainly characterized by sedimentary terrain, ranging from the Barremian at the base to the Quaternary at the top. El Ghrous perimeter is characterized by a Quaternary formation, with several levels of encrusted glacis (gypsum and limestone): it includes the calcareous, chalky, sandy and clayey alluviums. Such formation, also called Deb-deb of the Quaternary (Drouiche et al., 2013; Mostephaoui et al., 2013; Abdennour et al., 2020), consists of chalk and limestone located around the oases.

The study area is part of the wide hydrogeological basin of northern Sahara. It comprises several aquifers of various importances by

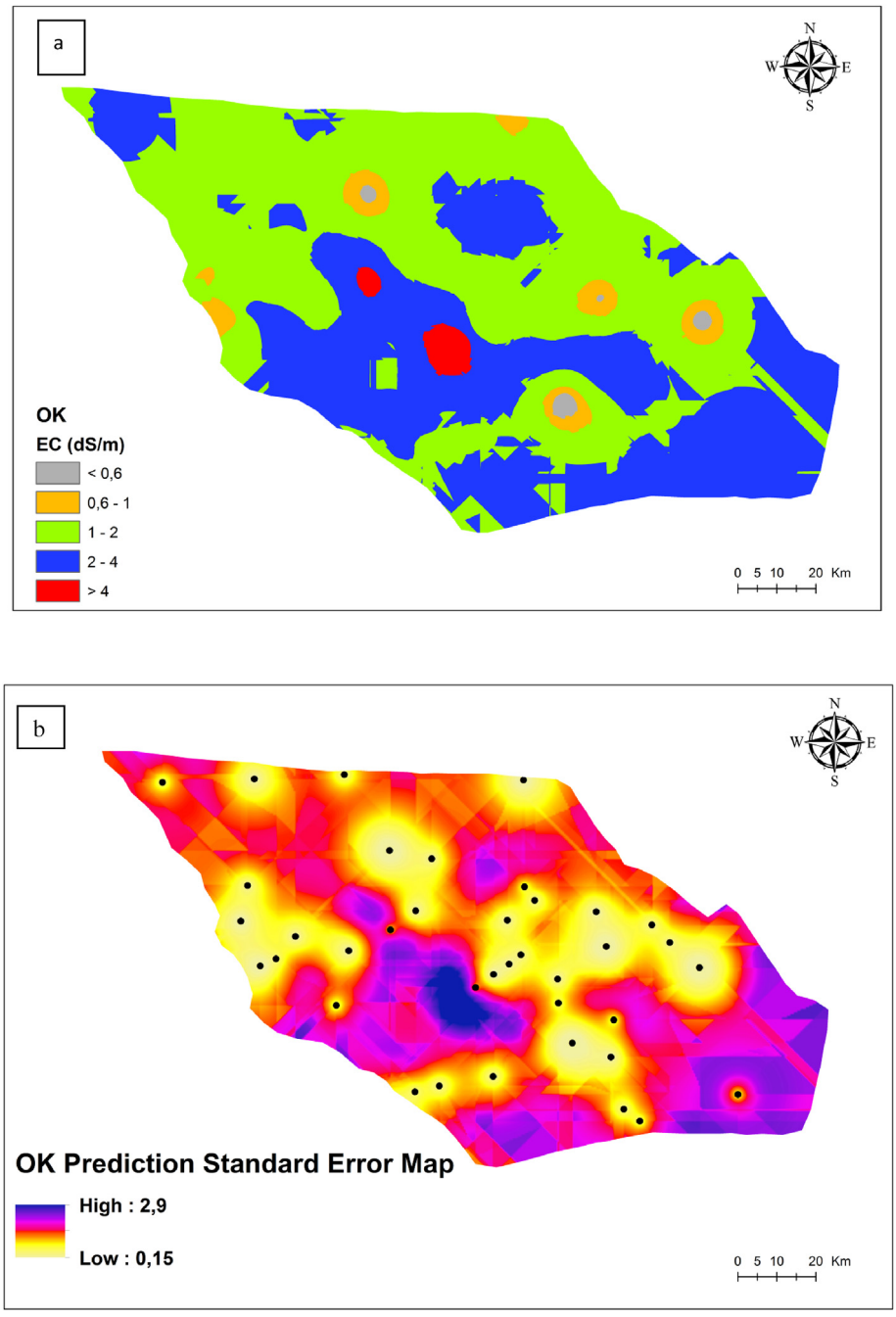

Fig. 5. Predicted map of EC by OK (a); Map of the standard estimation error (b).

Table 4
Parameters of variogram models for EC.

	Model	Range (m)	Sill	Nugget effect	Ratio (%)
OK	Spherical	1250	0.09	0.48	18.75
CK	Exponential	1000	0.015	0.43	3.78
CK_30	Exponential	1100	0.049	0.28	17.50
CK_35	Pentaspherical	1050	0.05	0.40	12.50
IK	Spherical	1400	0.17	1.53	11.11

lithological composition, geological structure and hydrogeological potentialities. Geophysical surveys, drillings, and the observations of stratigraphic columns allowed to identify different aquifers exploited in the Biskra region (Abdennour et al., 2020). According to Drouiche et al. (2013), the main aquifers exploited in the El Ghrous region belong to the following regional water bodies:

- Mio-Pliocene tablecloth: exploited mainly in the south of the region, where its thickness becomes considerable. It consists essentially of an alternation of impermeable clay layers and sand and gravel layers.
- Lower Eocene tablecloth: outcropping in the north of the region, becomes increasingly deeper southwards. Its reservoir is made of limestones and marly limestones. Various drillings showed that the Eocene limestones exhibit a dense network of diaclases often karstified. This aquifer is intensively expoloited and extends from the north to the centre of the region.

El Ghrous region is famous for its dates and for its vegetables crops in greenhouses, where three production systems are dominant: a date production system, vegetables crops system and a mixed system (dates and vegetables crops).

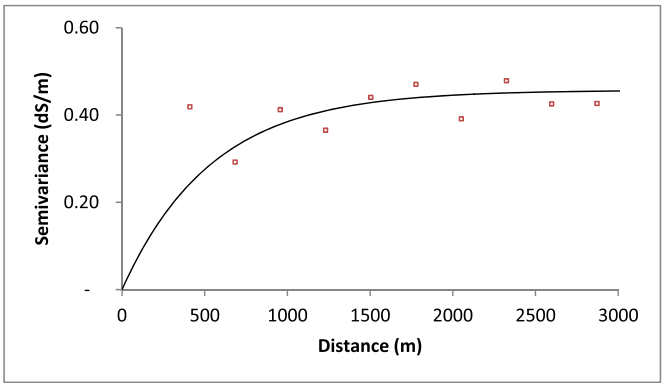

Fig. 6. Omnidirectional variogram of the predicted EC (CK).

According to Abdennour et al. (2019a), in the region a significant increase of the plasticulture sector (production of legumes in greenhouses) was observed across the period from 2009 to 2017, even if only 30% of the initial area was retained. This phenomenon is justified by the spreading of this production chain in space and over time, leading to a decline in soil fertility, namely the degradation caused by the increased use of saline irrigation water, which pushes farmers to move to other places to ensure better production (Abdennour et al., 2019a).

2.2. Soil sampling and laboratory analysis

Sampling was carried out in the period from October to November 2017 in 42 points (Fig. 1) in the soil of the palm groves of El Ghrous, to measure EC among other physico-chemical parameters. The exact position of each sampling point was determined by a handheld GPS. Soil samples were taken from the topsoil layer (0–15 cm), where salt accumulation was expected to be high.

As a pre-treatment, soil samples were dried in open air and sieved at 2 mm, then packed in plastic bags and analysed in the soil science laboratory of the Scientific and Technical Research Centre on Arid Regions (Biskra, Algeria), adopting standard procedures (Rodier et al., 2009). Since the physical characteristic of the soil (sandy texture) did not allow us to easily determine the saturation history of the soil samples - due to the difficulties encountered in identifying the saturation criteria of the paste (Semar et al., 2019) - EC is measured by the electrical method on a 1:5 aqueous extract. Such extract has the advantage of simplicity, reducing time and cost compared to saturation pulp extracts (Franzen, 2007). The measured values were adjusted to a temperature of 25 °C.

Methods adopted for soil solution analyses were described by Aubert (1978). The main cations (Ca^{2+}, Mg^{2+}, Na^{+} and K^{+}) and anions (Cl^{-}, NO_{3^-}, $HCO3^-$ and $SO4^{2-}$) were analysed. All cations and anions were processed by PHREEQC software for geochemical modelling of saturation indices.

Geochemical modelling of solutions was performed with the PHREEQC 2.12 geochemical code. The saturation mineral index (aragonite, calcite, gypsum, and halite) was examined by calculating the SI, which is expressed as follows (Parkhurst and Appelo, 2005):

$$SI = \log (IAP/Ks) \quad (1)$$

where IAP is the product of ionic activity, and Ks is the solubility constant of the mineral. If groundwater is saturated by a particular mineral species, then SI = 0 (steady state), whereas SI > 0 indicates supersaturation relative to the mineral species (precipitation state), and SI < 0 indicates undersaturation (dissolution state) (Zaidi et al., 2017).

2.3. Terrain parameters and Normalized Difference Vegetation Index

The Shuttle Radar Topography Mission (SRTM) is one of the most important surveys in Earth's space. In this study, the elevation of the Biskra area was extracted from the SRTM image using Arc-GIS 10.5 software (Fig. 1). A Digital Elevation Model (DEM) can be used in various ways to study soil salinity in arid areas. In addition to land surface elevation, the DEM can be used to extract multiple attributes from the topography and predict soil properties (Bakr and Ali, 2019). From the DEM, the slope (in percent), was delineated using the spatial analysis tools in ArcGIS 10.5. Topographic information was extracted for all sampling points on the raster maps of each topographic parameter. The irrigated perimeter has a surface area of 93.24 Km^2, altitude ranging from 130 m to 216 m, and slope gradient ranging from 0.014% to 14%.

The Normalized Difference Vegetation Index (NDVI), which could distinguish the presence of green vegetation, was calculated as the normalized transformed ratio between the reflectance measured at the red wavelength range and Near InfraRed (NIR) wavelength range using the following formula (Rouse et al., 1974):

$$NDVI = (NIR\text{-}RED)/(NIR + RED) \quad (2)$$

2.4. Soil type and salinity classification

According to the Soil Map of Algeria, El Ghrous is dominated by alluvial soils and soils originated by wind erosion. Most of them contain sulfates in the topsoil, generally with light grey color and sometimes beige. Their structure is often crumbly, and a gypsum embedding with calcareous clusters or nodules are present.

In this study, we considered five salinity classes for soil (Durand 1983): C1, non-saline (EC = 0–0.6 dS m^{-1}); C2, slightly saline (EC = 0.6–1 dS m^{-1}); C3, moderately saline (EC = 1–2 dS m^{-1}); C4, very saline (EC = 2–4 dS m^{-1}); C5, extremely saline (EC > 4 dS m^{-1}).

2.5. Predictive mapping

According to Castrignanò et al. (2002), one of the major advantages of geostatistical mapping is the possibility of creating error maps and probability maps. Variography and Kriging are the two key tools for the geostatistical analysis. In this work OK and CK techniques were used to predict the spatial variability of EC, and to test the ability of auxiliary variables to improve the predictions.

The first step of a geostatistical analysis is the definition of the structure of the spatial variation by variogram (or co-variogram) estimation (Juan et al., 2011a). According to Arslan (2012) and Bradai et al. (2016), the variogram γ(h) represents the semi-variance of the difference between attribute values for all points separated by a lag distance. There are three parameters of variogram function: nugget, range, and sill. It is usually calculated with the following equation:

$$\gamma\left(h\right) = \frac{1}{2N(h)} \sum_{i=1}^{N(h)} [Z(x_i) - (Z(x_i + h)]^2 \quad (3)$$

where γ(h) is the experimental semivariance value for all pairs separated by a distance *h* (lag); Z (x_i) is the value of the considered variable in each point; Z ($x_i + h$) is the value of the variable in points at a discrete distance *h*; x_i represents the position where each Z (x_i) value was measured; N(h) represents the number of pairs of observations per distance h (Delhomme, 1978).

The spatial dependence can be classified based on the nugget/sill ratio (%). A ratio <25% indicates high spatial dependence, a ratio of 25–75% indicates moderate spatial dependence, and a ratio >75% indicates low spatial dependence (Cambardella et al., 1994; Arslan, 2012; Bradaï et al., 2016; Abdennour et al., 2019b).

In this study we applied three types of Kriging: two parametric methods – OK and CK – and a third non-parametric one – IK. The first method was used to make a predicted map of EC using only the measured sampling points, in the second one some covariates were introduced to

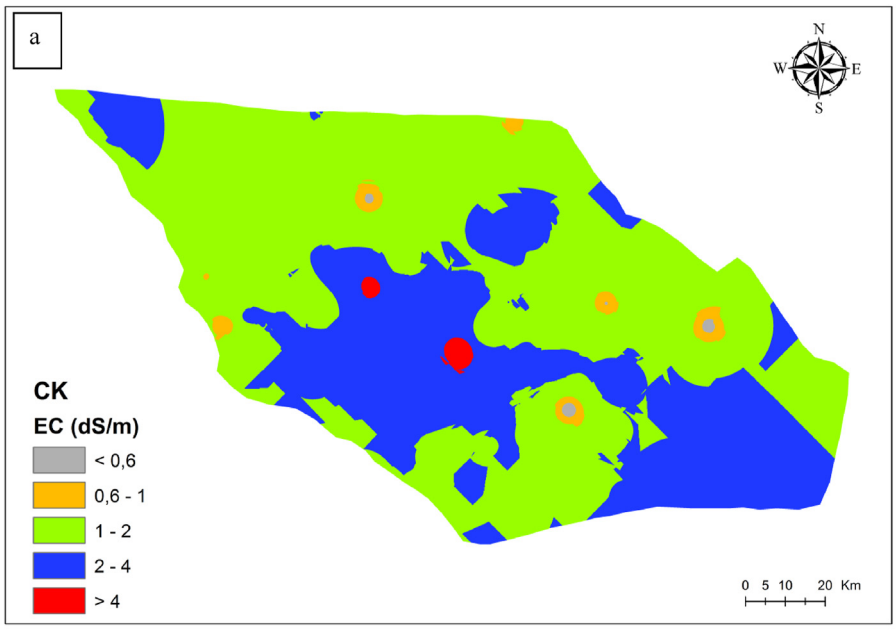

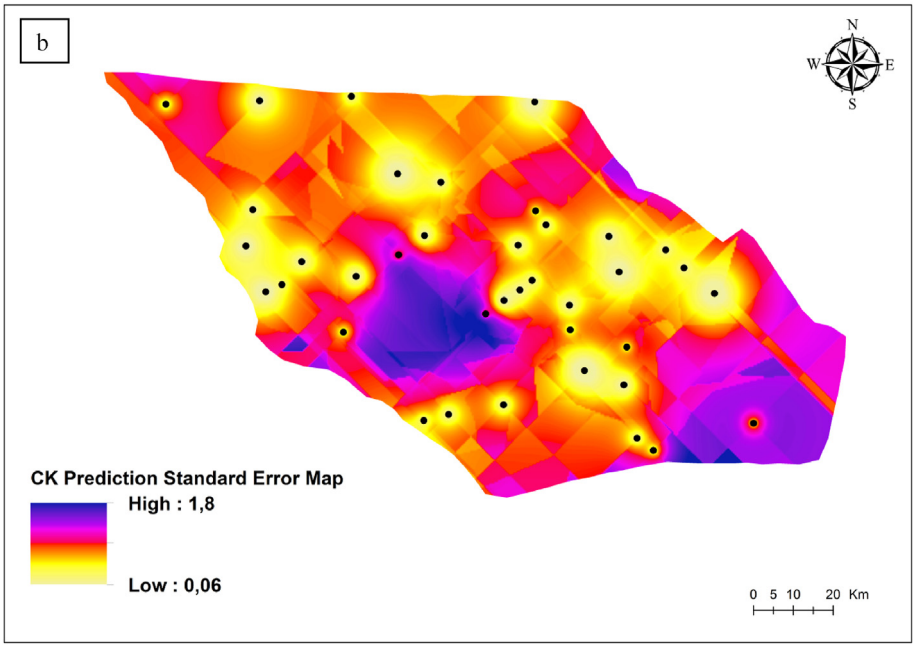

Fig. 7. Predicted map of EC by CK (a); Map of the standard estimation error (b).

improve the quality of the estimate, and finally the third was used to identify areas with a high susceptibility to salinization.

2.5.1. *Mapping by Ordinary Kriging*

OK, one of the most common and powerful geostatistical techniques, was already used to interpolate soil EC (Fourati et al., 2017). Such method is a commonly used linear spatial interpolator that provides estimates of variables at unsampled locations using information from neighboring points and assigning weights to these points as a function of their distance from the estimated point spatial variability structure (Bilgili, 2013).

$$Z^*(x0) = \sum_{i=1}^{n} \lambda i \, Z(x_i) \quad (4)$$

where Z *(x0) is the estimated value at the location x0, λi is the weight attributed to the i observation Z (xi), and n is the number of sites in the neighborhood search for estimation, based on the size of the mobile window which is user-defined. The weights are assigned to each sample so that the estimation variance is minimized and the estimates are unbiased (Webster and Oliver, 2007).

2.5.2. *Mapping by cokriging*

CK works best when the target variable is sampled less densely than the others (Eldeiry and Garcia, 2010). In this work, the CK method is used to improve the estimation of the primary variable (EC) introducing variables well correlated with the target variable (Isaaks and Srivastava, 1989). EC, SIg, elevation, and SO_4^{-2} are considered as primary, secondary, tertiary and quaternary variables in CK

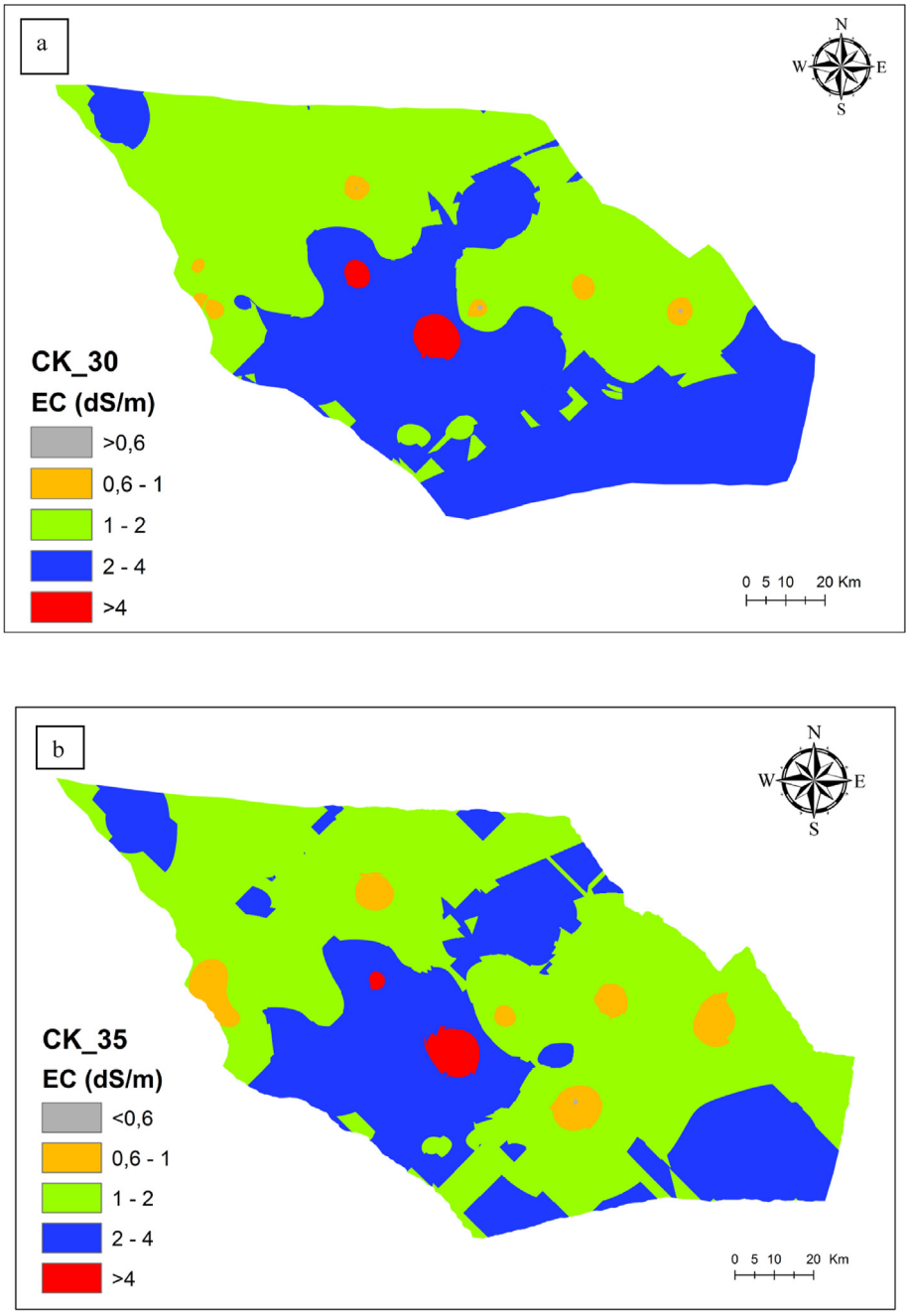

Fig. 8. Predicted map of EC by CK; a:with 30 samples; b: with 35 samples.

Table 5
Cross validation results for EC.

	ME	RMSE	Ratio (%)
OK	0.09	1.53	18.75
CK	0.004	0.92	3.78
CK_30	0.005	1.15	17.50
CK_35	−0.05	1.03	12.50
IK	0.01	0.44	11.11

interpolation, respectively. In fact, CK uses not only the spatial information on the primary variable but also the correlation between the variable of interest and the auxiliary variable to produce the interpolated map (Eldeiry and Garcia, 2010; AbdelRahman and Tahoun, 2019; Zhao et al., 2019). Unlike OK, the CK technique was used to perform an estimate of EC based on correlated data: terrain attributes are the most commonly used auxiliary variables in EC mapping with spectral indices from remote sensing (Bilgili, 2013; Taghizadeh-Mehrjardi et al., 2014; Yahiaoui et al., 2015; Li et al., 2019). In this study, terrain attributes (elevation and slope) were derived from DEM (Shuttle Radar Topography Mission ver.2, SRTM) with a ground resolution of 30 m. A Landsat 8 OLI TM satellite image of the area was acquired on October 31, 2017 (atmospheric correction was performed using the FLAASH module, implemented in ENVI 5.3 software), and used to calculate the NDVI. Variables that were significantly correlated with EC were used as covariates in the CK interpolation.

2.5.3. *Mapping by Indicator Kriging*

IK is a non-parametric geostatistical method for estimating the probability that the value of an attribute is not greater than a specific threshold, Z_c, at a given location U (Goovaerts et al., 1997). In IK, the numerical variable Z(u) is transformed into an indicator variable with a

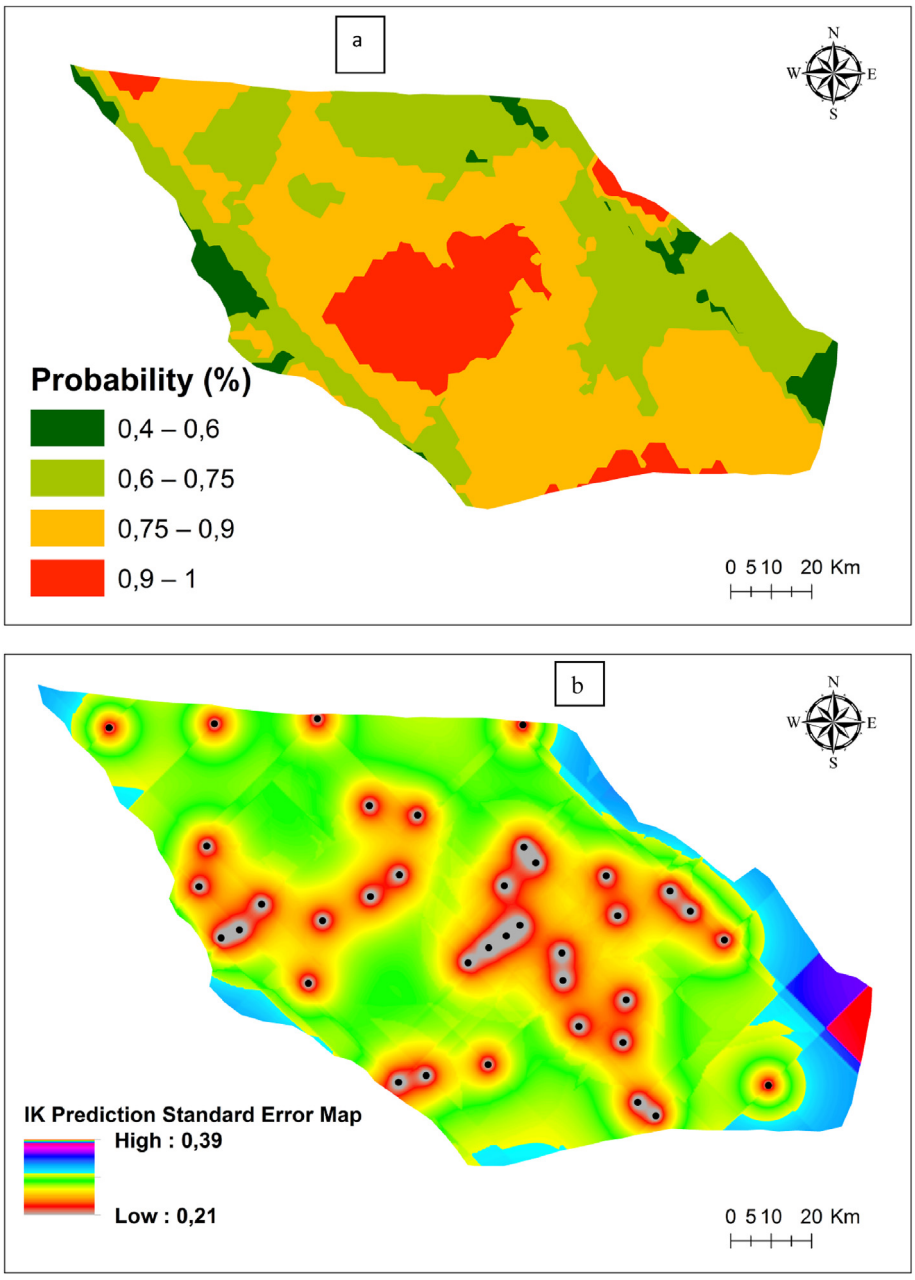

Fig. 9. Predicted map of EC by IK (a); Map of the standard prediction error (b).

Table 6
Comparison of the surface area obtained by OK and CK for each class.

Classes	C1	C2	C3	C4	C5
Area (Km^2) OK	0.26	1.82	57.60	32.91	0.65
Area (Km^2) CK	0.10	0.78	67.56	24.53	0.27

binary response, as follows:

$$I(x_i; Z_c) = \begin{cases} 1 & if Z(x_i) \geq Z_c \\ 0 & if Z(x_i) < Z_c \end{cases} \quad (5)$$

where I (x_i; Zc) is the value of the indicator at a location x_i; $Z(x_i)$ is the measured value at a location x_i; and $Z_c$is the threshold value. The expected value of I (x_i; Z_c), conditioned by *n* surrounding data, can be expressed as follows:

$$E[I(x_i; Z_c)] = Prob[Z(x) \leq Z_c]] = F(x_i; Z_c) \quad (6)$$

where F ($x_i Z_c$) is the conditional cumulative distribution function (CCDF). The function F represents the probability for an unknown value to not exceed a given threshold Zc. CCDFs are modeled using IK (Eldeiry and Garcia, 2011). This application produces a spatial distribution of the probability of exceeding a threshold, making it possible to generate maps representing the lines with the same probability (Piccini et al., 2012).

2.6. Validation and prediction accuracy

In order to assess the accuracy of the maps, the: mean error (ME) and the root mean square error (RMSE) were calculated from the values obtained by a cross-validation procedure. For a good prediction, ME should be close to 0 (Arslan, 2012; Fourati et al., 2017). If the model accurately describes the data, the RMSE should have approximately the same order of magnitude of the standard deviation (Piccini et al., 2014).

ME and RMSE were estimated using the following formulas:

$$ME = \frac{1}{n}\sum_{i=1}^{n} Z^{*}(xi) - Z\ (xi) \quad (7)$$

$$RMSE = \sqrt{\sum_{i=1}^{n} \frac{1}{n}[Z^{*}(xi) - Z(xi)]^{2}} \quad (8)$$

where Z*(xi) is the predicted value; Z(xi) is the measured value; and *n* is the number of validation points .

3. Results and discussion

A statistical description of the physico-chemical parameters of soils is given in Table 1 and Table 2. The EC varies from 0.45 to 6.5 dS m^{-1}, with an average of 1.85 dS m^{-1}. The coefficient of variation is 47.36%, showing the spatial heterogeneity of EC in the soils of this region. The pH of the soil samples was slightly alkaline (pH > 7.5). In some samples, it can reach high values. It varies from 7.7 to 8.9 with an average value of 8.12. The coefficient of variation (CV) was remarkable for all the parameters, which explains the spatial heterogeneity of the soil in this area.

It is commonly accepted that soils from arid (and semi-arid) areas in which irrigation agriculture is practiced have a significant risk of salinization, evidenced firstly by high pH values. In El Ghrous, for instance, most of the measured values are beyond the limits that Aubert (1983) proposed as thresholds for land degradation (pH: 8.0–9.0). Secondly, the EC values can better indicate the salinization effects. Our values showed a great variability, indicating a great spatial heterogeneity in the region: 75% of our samples overcame the threshold of 1.0 dS m^{-1} proposed by Durand (1983) as the point from which salinization begins to be a problem for land management.

The average measured concentrations of the main cations and anions of the samples is the order of magnitude: $Ca^{2+} > Na^{+} > Mg^{2+} > K^{+}$ and $SO_4{}^{2-} > Cl^{-} > HCO_3{}^{-}$. Ca^{2+} is the dominant cation and $SO_4{}^{2-}$ the dominant anion. Calcium is ranging from 8 to 76 meq/l with an average of 32.23 meq/l. Sulfate, which is the dominant anion in all samples, varies from 2.8 to 50 meq/l, with an average of 14 meq/l. The predominance of Ca^{2+} and SO_4^{2-} in the soil samples seems to be due to the dissolution of evaporation salts such as calcite, gypsum and anhydride (Lotfi et al., 2018).

The coefficients of variation for EC, Ca^{2+} and $SO_4{}^{2-}$, are very high. This explains the heterogeneity in the soils of the study area.

The saturation state of the soil samples was analysed using the PHREEQC hydrogeochemical equilibrium model (Parkhurst and Appelo, 2005). Fig. 2 shows the SI values of the soil samples studied.

Almost all samples are supersaturated in carbonatic minerals (aragonite, calcite), while evaporitic minerals (gypsum and halite) are undersaturated. Thus, carbonatic minerals are likely to precipitate, whereas sulfate minerals are always in an undersaturated state and therefore likely to dissolve. Their dissolution would contribute largely to the acquisition of the soil's salt charge. Dissolved gypsum could explain the enrichment in sulfate and calcium. The evaporitic minerals are still in an undersaturation state, which would allow their main ions (Cl^{-} and SO_4^{2-}) to appear in the soil solution with high concentrations. This was already confirmed by the dominant chemical facies ($CaSO_4$). Since halite (NaCl) is largely undersaturated in all the samples ($-5.41 > IS > -7.59$), it can dissolve and contribute to an increase in mineralization.

Most of the analysed soil samples resulted undersaturated for sulphur minerals (gypsum), with the exception of a limited number of samples whose SI for gypsum (SIg) was close to saturation. This suggests that gypsum dissolution was the source of Ca^{2+} and SO_4^{2-} in these soils. Modelling was carried out [Fig. 3 (a) and (b)] between salinity (EC) and the saturation index Gypsum, and between the sum of the parameters resulting from the dissolution of the gypsum ($Ca^{2+} + SO_4^{2-}$) and EC (Eq. (9)), which has a remarkable influence on the dominant facies for most soils.

$$CaSO_4{\cdot}2H_2O \rightarrow Ca^{2+} + SO_4^{2-} + 2H_2O \quad (9)$$

The correlation coefficient, which describes the relationship between EC and SIg, was 0.87, and the R^2 was 0.75, indicating that 75% of the EC variability can be explained by gypsum dissolution (SIg). Based on the geochemical characterization of soils, and the strong correlation between EC and gypsum dissolution, SIg and SO_4^{2-} were chosen as auxiliary variables for the estimation of soil salinity in CK.

A normality test (Kolmogorov-Smirnov) was performed to verify the normal distribution of soil EC data. The asymmetry and flattening (kurtosis) values were 1.75 and 6.62 respectively, which confirms the non-normal distribution of the data used. For this purpose, the values were transformed into logarithm before applying geostatistics.

Before applying Kriging, the dataset was checked for anisotropy: the variables showed the same spatial autocorrelation structure in all directions, meaning that the semivariance depends only on the distances among the sampling points (Amelung et al., 2006; Piccini et al., 2014). All optimized variograms were omnidirectional (isotropic) with no directional dependence. Experimental variograms were calculated, adopting a lag of 650 m. Then, theoretical spatial variability models were fitted to the experimental variograms by minimizing the sum of squares between experimental and model values (Lark, 2000; Marchetti et al., 2012). Parameters of the best variogram models were used in the Kriging interpolation.

3.1. OK application

The variogram model chosen was selected as the best fit for this type of Kriging. The experimental omnidirectional variogram of the EC soils (Fig. 4) indicates that the Spherical model was more suitable. The nugget effect (C_0) was 0.09 (dS m^{-1})^2, the presence of a high nugget value refers to measurement error, sampling error, inter-sample error (Burgos et al., 2006). The nugget value indicates that sampling and measurements were correctly performed. The sill (C_0+C) was 0.48(dS m^{-1})^2, and the range was 1250 m (Table 4).

The value of the nugget/sill ratio was 18.75%, indicating that soil EC in the El Ghrous region has a high spatial dependence (Cambardella et al., 1994).

Soil EC map estimated by OK is shown in Fig. 5a. It can be seen that the class 1 < EC < 2 dS m^{-1} is largely dominant in the study area. Such class is considered as moderately saline, thus these soils should be used with great care as the presence of salts has an effect on the plants. In the south-western part of the study area, the class 2 < EC < 4 dS m^{-1} indicates a very high degree of salinity. The most favorable class in this area is the one with EC < 1 dS m^{-1}, observed only as spots in a low percentage of the surface area.

3.2. CK application

Table 2 shows the Pearson's correlation coefficient between EC and the chemical parameters determined in this study. EC was significantly correlated ($p < 0.05$) to the calcium content ($r = 0.69$) and sulfate content ($r = 0.74$), while other parameters such as bicarbonate and potassium showed low correlation with EC.

Table 3 shows the correlation between EC and the available terrain parameters (elevation and slope), and NDVI (in this zone, NDVI ranged from 0.06 to 0.74). Only the elevation showed a significant correlation with soil EC, although the degree of correlation was relatively poor.

The maximum number of co-variables accepted by CK in ArcGIS 10.5 is three. Based on the results of the correlation between EC and the other soil parameters, we have chosen the most correlated ones (SIg. SO_4^{2-}. elevation) to be used as covariates in CK. The best fit for the cross variogram for EC (Fig. 6) was the exponential model. whose parameters are reported in Table 4. The nugget was 0.015; the sill was 0.43, the range was 1000 m. The value of the nugget/sill ratio indicate a high spatial dependence of the calculated EC.

Before introducing elevation as a covariate, we tried to construct a soil salinity distribution map by applying CK with only two covariates (SIg and SO_4^{-2}), which gave better results compared to OK. Despite the low correlation between EC and elevation ($r = -0.2$), incorporating this last variable further improved the estimate (Fig. 7).

CK is useful for reducing the sampling density, and improves the quality of the estimates (Kiani et al., 2020). We tried to use CK with a reduced number of samples, making a comparison with the map obtained by OK to test the efficiency of this technique. We developed two maps for EC (Fig. 8) with only 30 and 35 samples by applying CK, using the same covariates.

The spatial distribution of EC classes obtained from a reduced number of samples is similar to the OK map, with an equally good accuracy (Table 5). CK with a reduced number of samples and with covariates has given encouraging results, and can be used when few direct measurements of the target variable are available, but there are many measurements of other related variables. Thus, using the spatial structure of auxiliary data to model the spatial structure of the target variable is possible. CK is more difficult to implement than other Kriging techniques but it can be more efficient if the spatial structures are correctly determined.

Both maps obtained by these two types of Kriging indicate that soils in this area are prone to salinization. For this reason, a third type of Kriging, IK (non-parametric), was applied to draw up a map of the probability of exceeding an EC threshold.

3.3. IK application

IK has been applied to develop a map of the probability that soil EC in El Ghrous exceeds a given threshold, adopting a value of 1 dS m^{-1}, according to Durand's (1983) classification of salinity. Beyond this limit real problems for soil and plants can arise. Measured EC values were converted into a discrete indicator variable, which assumes a value of "1″ when the real value equals or exceed the threshold, or "0″ when the real value is below the threshold. After a variographic analysis of this variable, a spherical model was fitted and its parameters, reported in Table 4, were used for IK. Fig. 9 shows the probability of exceeding the threshold of 1 dS m^{-1}.

According to the study conducted by Bradai et al. (2016), we chose the probability of 50% as the level of significance. More than 93% of the study area exceeded the threshold. Then, Fig. 9 indicates that most soils in this area are affected by salinization, due to the increased use of groundwater for irrigation, often of mediocre quality. This situation is surely worrying and alarming, and this region urgently needs suitable hydrological and agricultural management practices which could help in rehabilitating soils. One of the best strategies for saline soil remediation is the proper selection of crops, not only for economic purposes. but also for the control of saline soil and water pollution (Niñerola et al., 2017).

Soil salinity is affected by precipitation, evaporation, water table. and topography in natural conditions (Xu et al., 2014; Yin et al., 2016). Moreover, the climatic conditions in southern Algeria, where evapotranspiration is very high, the poor quality of groundwater and inappropriate human agricultural activities have led to the risk of secondary soil salinization (Emadi and Baghernejad, 2014).

Overall, the salty soils in the study area require interventions aiming to stop salt accumulation, and a remediation process to prevent the spreading of soil salinization. The probability map by IK would be useful for local authorities to define and evaluate the agricultural land management strategy in the forthcoming PNDA (National Agricultural Development Plan) projects, with the aim of creating new sub-areas in the irrigated perimeters, and for the agricultural land management plan, identifying the vulnerable areas. Also the maps obtained by OK and CK could be used as effective tools for managers, to establish a management plan for minimizing salinization of these soils, and for developing a strategy to protect the crops.

The effectiveness of current irrigation practices and leaching activities must be carefully improved when the soil pH and EC exceed critical levels. First, a better management of irrigated soils and more efficient drainage techniques should be applied to reduce the spread of salinization, which threatens the agriculture and the economy of this region. In addition, the control and regulation of groundwater exploitation would reduce the risk and guarantee the sustainability of dates and vegetables production.

3.4. Models accuracy and comparison

Figs. 5 and 7 show the distribution maps of EC in the study area using OK and CK interpolation methods. Although both maps show a similar distribution pattern, the CK map delocalized small areas around the extreme EC values (EC > 4 and EC < 1 dS m^{-1}) better than the OK map.

The nugget/sill ratio of the three CK models is lower in comparison with the OK model, meaning that applying this type of kriging allows for lower error, stronger spatial autocorrelation, and lower range. These results are confirmed by the ME and RMSE values of the cross-validation.

A cross-validation (Table 5) of the OK and CK estimates was carried out to define the best model for predicting the distribution of EC in the El Ghrous perimeter. The cross validation showed the degree of accuracy of the predictions. ME was always close to zero but lower for CK. RMSE was smaller than standard deviation in both maps, but lower for CK. For IK, cross-validation showed that ME was close to 0, and RMSE value was low (0.44), meaning that the estimate is good.

From the prediction errors reported in Table 5 it is clear how CK outperformed OK in predicting EC: CK, after introducing other parameters into the EC estimation, gave a lower ME and RMSE (0.004 and 0.92). This confirms the usefulness of this technique for prediction. The results of this work have shown that interpolations based only on measured data may not be accurate enough, and may not truly represent the actual state of the EC. Adding other variables to the interpolation model, as in CK, could give higher prediction accuracy and thus deliver better results.

The spatial distribution of EC classes is further described in Table 6. The low class (EC < 0.6) dropped from 0.26 Km^2 with OK to 0.1 Km^2 with CK, meaning that this class was overestimated by OK. The same happened for the high class (EC > 4). According to Douaoui et al. (2006), there is a sort of prediction problem using OK, in particular with the extreme values. This result was also confirmed by Bradai et al. (2015).

The CK model produced a map with more similarities to the EC descriptive statistics from the soil samples, meaning that this technique had greater accuracy in describing the spatial variation of the EC. The mean values (1.75 dS m^{-1}) and standard deviation (0.79) are also closer to the values for the soil samples (1.9 and 0.9 dS m^{-1} respectively). In this work, the comparison of the OK and CK performances in EC prediction confirm the findings of Tajgardan et al. (2010), Ashrafzadeh et al. (2016) and Bogunovic et al. (2017). Other studies, e.g. Boubehziz et al. (2020), reported that the performance of OK in predicting soil organic carbon in northeast Algeria is poor, thus they opted for another type of Kriging.

The CK method has demonstrated to be a more robust interpolation method. provided that the auxiliary variables are well correlated with the target soil property (Wu et al., 2009). Gypsum is the main constituent of the soil salts in this area, and being correlated to EC. SO_4^{2-} and SIg were used as covariates. There was also a significant negative correlation between elevation and EC. Thus, interpolating EC by CK with Sig, SO_4^{2-} and elevation as auxiliary variables proved to be a robust way to improve the accuracy of predicting soil conditions in this study.

Standard error maps allow to know the prediction error in each point of the map, thus are useful to check the model, and eventually to correct the sampling strategy. Standard error maps for EC obtained by CK and OK show a spatial distribution that is very sensitive to sampling density. Areas with low sampling density show a lower estimation quality, while areas with higher sampling density show a better quality of the estimate.

4. Conclusions

The El Ghrous region, mainly occupied by agricultural land, has an important economic value for Algeria. Monitoring and assessing the

spatial distribution of soil salinity is very important for soil sustainability. The utilized Kriging techniques showed how the area suffers from salinization. Application of the OK and CK methods to interpolate the EC in non-sampled locations from sampled points provided distribution maps with acceptable error, but an improvement in the interpolation accuracy was obtained using CK. CK is used when few measurements are available for the target variable, but there are many measurements of other related variables. Thus, it is possible to use the spatial structure of auxiliary data to model the spatial structure of the target variable, especially if this last is expensive to measure. A geostatistical analysis revealed that the distribution of EC in our study area was correlated with the elevation of the region, gypsum saturation index, and sulfate content.

Application of IK showed that 93% of the study area exceeds the threshold value of 1 dS m^{-1}, which represents the minimum threshold for soil salinity. This is very alarming, and requires follow-up and a rapid response plan to deal with this situation. On the basis of the EC distribution maps, some recommendations can be made to control agricultural production. These maps could then represent a decision support tool for land managers to take the correct measures, such as raising farmers' awareness or possible development plans: installation of drainage networks, choice of crops according to salinity tolerance. In summary, the use of geostatistical methods for mapping and managing salinity in irrigated agriculture is crucial, for minimizing its negative environmental impacts and for ensuring the long-term sustainability of agriculture.

Declaration of competing interest

The authors declare that they have no known competing financial interests or personal relationships that could have appeared to influence the work reported in this paper.

References

AbdelRahman, M.A., Tahoun, S., 2019. GIS model-builder based on comprehensive geostatistical approach to assess soil quality. Remote Sensing Applications: Society Environment 13, 204–214.

Abdennour, M.A., Douaoui, A., Barrena, J., Pulido, M., Bradaï, A., Bennacer, A., Piccini, C., Alfonso-Torreño, A., 2020. Geochemical characterization of the salinity of irrigated soils in arid regions (Biskra, SE Algeria). Acta Geochimica. https://link.springer.com/article/10.1007%2Fs11631-020-00426-2.

Abdennour, M.A., Douaoui, A., Bennacer, A., Manuel, P.F., Bradai, A., 2019a. Detection soil salinity as a consequence of land cover changes at El Ghrous (Algeria) irrigated area using satellite images. Agrobiologia 9, 1458–1470.

Abdennour, M.A., Douaoui, A., Bradai, A., Bennacer, A., Pulido Fernández, M., 2019b. Application of kriging techniques for assessing the salinity of irrigated soils: the case of El Ghrous perimeter, Biskra, Algeria. Spanish Journal of Soil Science 9, 105–124.

Adimalla, N., Taloor, A.K., 2020. Hydrogeochemical investigation of groundwater quality in the hard rock terrain of South India using Geographic Information System (GIS) and groundwater quality index (GWQI) techniques. J Groundwater for Sustainable Development 10, 100288.

Afrasinei, G.M., Melis, M.T., Buttau, C., Bradd, J.M., Arras, C., Ghiglieri, G., 2017. Assessment of remote sensing-based classification methods for change detection of salt-affected areas (Biskra area, Algeria). J. Appl. Remote Sens. 11, 016025.

Amelung, W., Zhang, X., Flach, K.J.G., 2006. Amino acids in grassland soils: climatic effects on concentrations and chirality. Geoderma 130, 207–217.

Arslan, H., 2012. Spatial and temporal mapping of groundwater salinity using ordinary kriging and indicator kriging: the case of Bafra Plain, Turkey. Agric. Water Manag. 113, 57–63.

Ashrafzadeh, A., Roshandel, F., Khaledian, M., Vazifedoust, M., Rezaei, M., 2016. Assessment of groundwater salinity risk using kriging methods: a case study in northern Iran. Agric. Water Manag. 178, 215–224.

Aubert, G., 1978. Méthodes d'analyses des sols. Centre national de documentation pédagogique, Centre régional de documentation pédagogique de Marseille in French.

Aubert, G., 1983. Observations sur les caractéristiques, la dénomination et la classification des sols salés ou salsodiques. Cah. O.R.S.T.O.M. Pedol. 20, 73–78.

Azadmard, B., Mosaddeghi, M.R., Ayoubi, S., Chavoshi, E., Raoof, M., 2018. Spatial variability of near-saturated soil hydraulic properties in Moghan plain, North-Western Iran. Arabian Journal of Geosciences 11, 452.

Bakr, N., Ali, R.R., 2019. Statistical relationship between land surface altitude and soil salinity in the enclosed desert depressions of arid regions. Arabian Journal of Geosciences 12, 715.

Bilgili, A., 2013. Spatial assessment of soil salinity in the Harran Plain using multiple kriging techniques. J Environmental monitoring assessment 185, 777–795.

Bogunovic, I., Pereira, P., Brevik, E.C., 2017. Spatial distribution of soil chemical properties in an organic farm in Croatia. Sci. Total Environ. 584, 535–545.

Boubehziz, S., Khanchoul, K., Benslama, M., Benslama, A., Marchetti, A., Francaviglia, R., Piccini, C., 2020. Predictive mapping of soil organic carbon in Northeast Algeria. Catena 190, 104539.

Boufekane, A., Saighi, O., 2016. Kriging method of study of the groundwater quality used for irrigation-case of Wadi Djendjen plain (North-East Algeria). J. Fund. Appl. Sci. 8, 346–362.

Bougherara, A., Lacaze, B., 2009. Etude preliminaire des images Landsat et Alsat pour le suivi des mutations agraires des Ziban (extrême nord-est du Sahara algérien) de 1973 à 2007. Journées d'Animation Scientifique de l'AUF in French.

Bradaï, A., Douaoui, A., Bettahar, N., Yahiaoui, I., 2016. Improving the prediction accuracy of groundwater salinity mapping using indicator Kriging method. J. Irrigat. Drain. Eng. 142, 04016023.

Burgos, P., Madejón, E., Pérez-de-Mora, A., Cabrera, F., 2006. Spatial variability of the chemical characteristics of a trace-element-contaminated soil before and after remediation. J Geoderma 130, 157–175.

Cambardella, C.A., Moorman, T.B., Novak, J., Parkin, T., Karlen, D., Turco, R., Konopka, A., 1994. Field-scale variability of soil properties in central Iowa soils. Soil Sci. Soc. Am. J. 58, 1501–1511.

Castrignanò, A., Maiorana, M., Fornaro, F., Lopez, N., 2002. 3D spatial variability of soil strength and its change over time in a durum wheat field in Southern Italy. Soil Tillage Res. 65, 95–108.

Chagas, C.d.S., Carvalho Júnior, W.d., Pinheiro, H.S.K., Xavier, P.A.M., Bhering, S.B., Pereira, N.R., Calderano Filho, B., 2018. Mapping soil cation exchange capacity in a semiarid region through predictive models and covariates from remote sensing data. J Revista Brasileira de Ciência do Solo 42.

Chebbah, M., 2016. A Miocene-restricted platform of the Zibane zone (Saharan Atlas, Algeria), depositional sequences and paleogeographic reconstruction. Arabian Journal of Geosciences 9, 151.

Dankoub, Z., Ayoubi, S., Khademi, H., Lu, S.-G., 2012. Spatial distribution of magnetic properties and selected heavy metals in calcareous soils as affected by land use in the Isfahan region, Central Iran. Pedosphere 22, 33–47.

Delhomme, J.P., 1978. Kriging in Hydrosciences. Adv. Water Resourc. 1 (5), 251–266.

Douaoui, A.E.K., Nicolas, H., Walter, C., 2006. Detecting salinity hazards within a semiarid context by means of combining soil and remote-sensing data. Geoderma 134, 217–230.

Drouiche, A., Chaib, W., Rezeg, A., Bougherira, N., 2013. Risque de contamination des eaux souterraines par les nitrates en régions arides; cas d'Elghrous (Région des Ziban-Sud-Est Algérien). No Special 2013, CRSTRA Journal Algérien des Régions Arides 65–75. in French.

Durand, J.H., 1983. The Irrigable Soils. Academic Press France, Paris.

Eldeiry, A.A., Garcia, L.A., 2010. Comparison of ordinary kriging, regression kriging, and cokriging techniques to estimate soil salinity using LANDSAT images. J. Irrigat. Drain. Eng. 136, 355–364.

Emadi, M., Baghernejad, M., 2014. Comparison of spatial interpolation techniques for mapping soil pH and salinity in agricultural coastal areas, northern Iran. Arch. Agron Soil Sci. 60, 1315–1327.

Florinsky, I.V., Eilers, R.G., Lelyk, G.W., 2000. Prediction of soil salinity risk by digital terrain modeling in the Canadian prairies. J Canadian Journal of Soil Science 80, 455–463.

Fourati, H.T., Bouaziz, M., Benzina, M., Bouaziz, S., 2017. Detection of terrain indices related to soil salinity and mapping salt-affected soils using remote sensing and geostatistical techniques. J Environmental monitoring assessment 189, 177.

Franzen, D., 2007. Salt Accumulation Processes. North Dakota state Univ., Fargo ND 58105.

Goovaerts, P., 1997. Geostatistics for Natural Resources Evaluation. Oxford University Press on Demand.

Goovaerts, P., Webster, R., Dubois, J.-P., 1997. Assessing the risk of soil contamination in the Swiss Jura using indicator geostatistics. Environ. Ecol. Stat. 4, 49–64.

Gorji, T., Sertel, E., Tanik, A., 2017. Monitoring soil salinity via remote sensing technology under data scarce conditions: a case study from Turkey. Ecol. Indicat. 74, 384–391.

Hengl, T., Toomanian, N., Reuter, H.I., Malakouti, M.J., 2007. Methods to interpolate soil categorical variables from profile observations: lessons from Iran. J Geoderma 140, 417–427.

Isaaks, E.H., Srivastava, M.R., 1989. Applied Geostatistics.

Juan, P., Mateu, J., Jordan, M., Mataix-Solera, J., Meléndez-Pastor, I., Navarro-Pedreño, J., 2011a. Geostatistical methods to identify and map spatial variations of soil salinity. J. Geochem. Explor. 108, 62–72.

Juan, P., Mateu, J., Jordan, M., Mataix-Solera, J., Meléndez-Pastor, I., Navarro-Pedreño, J., 2011b. Geostatistical methods to identify and map spatial variations of soil salinity. J Journal of Geochemical Exploration 108, 62–72.

Kiani, M., Hernandez-Ramirez, G., Quideau, S.A., 2020. Spatial variation of soil quality indicators as a function of land use and topography. J Canadian Journal of Soil Science 1–16.

Lark, R., 2000. A comparison of some robust estimators of the variogram for use in soil survey. Eur. J. Soil Sci. 51, 137–157.

Lark, R., Ferguson, R., 2004. Mapping risk of soil nutrient deficiency or excess by disjunctive and indicator kriging. Geoderma 118, 39–53.

Li, Z., Li, Y., Xing, A., Zhuo, Z., Zhang, S., Zhang, Y., Huang, Y., 2019. Spatial prediction of soil salinity in a semiarid oasis: environmental sensitive variable selection and model comparison. J Chinese Geographical Science 29, 784–797.

Long, X.-H., Zhao, J., Liu, Z.-P., Rengel, Z., Liu, L., Shao, H.-B., Tao, Y., 2014. Applying geostatistics to determine the soil quality improvement by Jerusalem artichoke in coastal saline zone. J Ecological engineering 70, 319–326.

Lotfi, D., Yann, L., Gerhard, S., Mohamed, H., Rajouene, M., 2018. Identifying the origin of groundwater salinisation in the Sidi El Hani basin (central-eastern Tunisia). J. Afr. Earth Sci. 147, 443–449.
Manning, G., Fuller, L.G., Eilers, R.G., Florinsky, I., 2001. Topographic influence on the variability of soil properties within an undulating Manitoba landscape. Can. J. Soil Sci. 81, 439–447.
Marchetti, A., Piccini, C., Francaviglia, R., Mabit, L., 2012. Spatial distribution of soil organic matter using geostatistics: a key indicator to assess soil degradation status in central Italy. Pedosphere 22, 230–242.
Mostephaoui, T., Bensaid, R., Saker, M.L., 2013. Localization and delimitation of the arid soils by remote sensing and in-situ measurements in an arid area: case of Oued Djedi watershed, Biskra, Algeria. World Appl. Sci. J. 24, 370–382.
Niñerola, V.B., Navarro-Pedreño, J., Lucas, I.G., Pastor, I.M., Vidal, M.M.J., 2017. Geostatistical assessment of soil salinity and cropping systems used as soil phytoremediation strategy. J. Geochem. Explor. 174, 53–58.
Norouzi, M., Ayoubi, S., Jalalian, A., Khademi, H., Dehghani, A.A., 2010. Predicting rainfed wheat quality and quantity by artificial neural network using terrain and soil characteristics. Acta Agric. Scand. Sect. B Soil Plant Sci 60, 341–352.
Odeh, I.O.A., Onus, A., 2008. Spatial analysis of soil salinity and soil structural stability in a semiarid region of new south Wales, Australia. Environ. Manag. 42, 265.
Parkhurst, D., Appelo, C., 2005. PHREEQC-2 Version 2.12: A Hydrochemical Transport Model. US Geological Survey Central Region Research, USGS Water Resources Division.
Piccini, C., Marchetti, A., Farina, R., Francaviglia, 2012. Application of indicator kriging to evaluate the probability of exceeding nitrate contamination thresholds. Int. J. Environ. Res. 6, 853–862.
Piccini, C., Marchetti, A., Francaviglia, R., 2014. Estimation of soil organic matter by geostatistical methods: use of auxiliary information in agricultural and environmental assessment. Ecol. Indicat. 36, 301–314.
Pozdnyakova, L., Zhang, R., 1999. Geostatistical analyses of soil salinity in a large field. Precis. Agric. 1, 153–165.
Rechachi, M.Z., 2017. Impact de la qualité des eaux d'irrigation sur la salinisation des sols en régions arides et semi arides: cas de la région du Ziban. Université Mohamed Khider-Biskra in French.
Rodier, J., Legube, B., Merlet, N., 2009. L'Analyse de l'eau 9e édition Entièrement Mise À Jour Dunod Paris in French.
Rouse, J., Haas, R., Schell, J., Deering, D., 1974. Monitoring Vegetation Systems in the Great Plains with ERTS, vol. 351. NASA special publication, p. 309.
Safarbeiranvnd, M., Amanipoor, H., Battaleb-Looie, S., Ghanemi, K., Ebrahimi, B., 2018. Quality evaluation of groundwater resources using geostatistical methods (case study: central Lorestan Plain, Iran). J Water Resources Management 32, 3611–3628.
Semar, A., Hartani, T., Bachir, H., 2019. Soil and water salinity evaluation in new agriculture land under arid climate, the case of the Hassi Miloud area, Algeria. Euro-Mediterranean Journal for Environmental Integration 4, 40.
Seyedmohammadi, J., Matinfar, H.R., 2018. Statistical and geostatistical techniques for geospatial modeling of soil cation exchange capacity. J Communications in Soil Science Plant Analysis 49, 2301–2314.
Taghizadeh-Mehrjardi, R., Ayoubi, S., Namazi, Z., Malone, B.P., Zolfaghari, A.A., Sadrabadi, F.R., 2016. Prediction of soil surface salinity in arid region of central Iran using auxiliary variables and genetic programming. Arid Land Res. Manag. 30, 49–64.
Taghizadeh-Mehrjardi, R., Minasny, B., Sarmadian, F., Malone, B., 2014. Digital mapping of soil salinity in Ardakan region, central Iran. J Geoderma 213, 15–28.
Tajgardan, T., Ayoubi, S., Shataee, S., Sahrawat, K.L., Gorgan, I., 2010. Soil surface salinity prediction using ASTER data: comparing statistical and geostatistical models. J Australian Journal of Basic Applied Sciences 4, 457–467.
Van Meirvenne, M., Goovaerts, P., 2001. Evaluating the probability of exceeding a site-specific soil cadmium contamination threshold. Geoderma 102, 75–100.
Vermeulen, D., Van Niekerk, A., 2017. Machine learning performance for predicting soil salinity using different combinations of geomorphometric covariates. Geoderma 299, 1–12.
Wang, Y., Deng, C., Liu, Y., Niu, Z., Li, Y., 2018. Identifying change in spatial accumulation of soil salinity in an inland river watershed, China. Sci. Total Environ. 621, 177–185.
Webster, R., Oliver, M.A., 2007. Geostatistics for Environmental Scientists. John Wiley & Sons.
Wu, C., Wu, J., Luo, Y., Zhang, L., DeGloria, S.D., 2009. Spatial estimation of soil total nitrogen using cokriging with predicted soil organic matter content. Soil Sci. Soc. Am. J. 73, 1676–1681.
Xu, Y., Pu, L., Zhu, M., Li, J., Zhang, M., Li, P., Zhang, J., 2014. Spatial variation of soil salinity in the coastal reclamation area, eastern China. J. Coast Res. 30, 411–417.
Yahiaoui, I., Douaoui, A., Zhang, Q., Ziane, A., 2015. Soil salinity prediction in the Lower Cheliff plain (Algeria) based on remote sensing and topographic feature analysis. Journal of Arid Land 7, 794–805.
Yin, A., Zhang, M., Gao, C., Yang, X., Xu, Y., Wu, P., Zhang, H., 2016. Salinity evolution of coastal soils following reclamation and intensive usage, Eastern China. Environmental Earth Sciences 75, 1281.
Zaidi, F.K., Al-Bassam, A.M., Kassem, O.M., Alfaifi, H.J., Alhumidan, S.M., 2017. Factors influencing the major ion chemistry in the Tihama coastal plain of southern Saudi Arabia: evidences from hydrochemical facies analyses and ionic relationships. Environmental Earth Sciences 76, 472.
Zhao, W., Cao, T., Li, Z., Sheng, J., 2019. Comparison of IDW, cokriging and ARMA for predicting spatiotemporal variability of soil salinity in a gravel–sand mulched jujube orchard. Environ. Monit. Assess. 191, 376.
Zolfaghari, Z., Ayoubi, S., Mosaddeghi, M.R., 2015. Spatial variability of some soil shrinkage indices in hilly calcareous region of western Iran. Soil Tillage Res. 150, 180–191.